Al-Mustansiriyah Journal of Science
ISSN: 1814-635X (print), ISSN:2521-3520 (online) Volume 34, Issue 3, 2023 DOI: http://doi.org/10.23851/mjs.v34i3.1369

Research Article **Open Access**

Plasma Parameters Diagnosis of Laboratory Ar/O_2 Cold Atmospheric Plasma Jet using Different Potential Discharges

Roonak Abdul-Salam Alkareem[1*], Baida M. Ahmed[1], Osama Abdul-Azeez Dakhil[1], Ali Albeer[2]

[1]Department of Physics, College of Science, Mustansiriyah University, 10052 Baghdad, Iraq.
[2]Biometry and epidemiology (IBE), Institute of medical information processing, Ludwig Maximilian University of Munich (LMU), Germany.

*Correspondent contact: roonak_1988@uomustansiriyah.edu.iq

Article Info

Received
12/04/2023

Revised
11/05/2023

Accepted
28/05/2023

Published
30/09/2023

ABSTRACT

This paper offers a clear methodology for the characterization of cold atmospheric plasmas and their development. The optical emission spectra of an Ar/O_2 plasma jet produced in a plasma jet system at constant flow rates and for various potential discharges between 14 kV and 18 kV revealed that variations in voltage caused a significant difference in the intensity of the Ar/O_2 emission. The plasma characteristics of electron temperature (T_e), electron density (n_e), plasma frequency (f_p), Debye length (λ_D), and the number of particles in the Debye sphere (N_D), were estimated using the technique of optical emission spectroscopy (OES). The obtained data are subject to further analysis and discussion. It was determined that potential discharges increased, and an electron temperature increased from 1.34 eV to 1.54 eV. With rising potential discharges, the Debye length decreases while the electron density, plasma frequency, and number of particles in the Debye sphere increase.

KEYWORDS: Plasma jet, AC plasma discharge, Ar/O_2 mixture, OES, plasma parameters.

الخلاصة

يقدم هذا البحث منهجية واضحة لوصف بلازما الغلاف الجوي البارد وتكوينها. كشفت أطياف الانبعاث البصري لبلازما النفث Ar / O_2 المنتجة بمعدلات تدفق ثابتة ولتفريغات الجهد المختلفة بين ١٤ و ١٨ كيلو فولت أن هناك تغيير كبير في شدة الأنبعاث Ar / O_2. تم تقدير خصائص البلازما لدرجة حرارة الإلكترون (T_e)، كثافة الإلكترون (n_e)، تردد البلازما (f_p)، طول ديباي (λ_D) ، وعدد الجسيمات في كرة ديباي (N_D) باستخدام تقنية التحليل الطيفي للانبعاثات الضوئية (OES). وجد ان بزيادة جهد التفريغ هناك زيادة في درجة حرارة الإلكترون من ١,٣٤ إلى ١,٥٤ فولت ، و تزداد كثافة الإلكترون, تردد البلازما وعدد الجسيمات في كرة ديباي بينما هناك انخفاض في طول ديباي.

INTRODUCTION

Last several decades, AC and DC cold atmospheric plasmas (CAPs) or non-thermal plasma (NTP) considered important in diverse fields such as food [1][2], biomaterial and biomedicine [3][4], material synthesis and processing [5][6], surface modification [7], thin film treatment [8], catalysts [9], and agriculture [10][11]. Thus CAPs have allowed the development of various sources of non-thermal plasma (NTP) close to room temperature, which allows previously impossible plasma applications [12]. Computational, experimental, and theoretical investigations of atmospheric pressure plasmas offer a range of compelling novel research insights into the fundamental aspects of these plasmas and their practical uses. CAPs eliminate the need for complicated and expensive vacuum equipment; Thus, it allows numerous innovative designs to meet the rising demand for reliable, cost-effective, and easy-to-operate plasma sources [13]. Among other CAPs, the non-equilibrium plasma jets have attracted great interest since they are generated in open space rather than in the space between two electrodes. The evolution of the plasma is also driven by non-equilibrium in the internal

levels and in the energy distribution of free electrons, which activates mechanisms that can effectively produce the desired particular reaction products [14][15]. The majority of CAPs used in bio-applications are produced by delivering electrical energy to plasma-forming gases (helium, argon, nitrogen, oxygen, or combinations of these gases), which at room temperature produce low-energy ions and hot-energy electrons [16]. The presence of O_2 in the plasma is important because it promotes the development of reactive oxygen species (ROS), which are crucial to the therapeutic action of CAPs [17, 18]. The ROS including superoxide (O_2^-), O, H_2O_2, OH radicals, and ozone (O_3) is produced by a non-thermal atmospheric plasma jet (NTAPJ) [19]. In NTAPJ, acceleration-induced electron-gas collision resulting excited or ionized gas depending on the energy of accelerated electrons [20][21]. However, the generation of ROS important for biomedical procedures like canal therapy, cancer treatment, wound healing, and surface sterilization [22][23].

Ionized and excited states have a vital role in plasma physics and chemistry. To make accurate simulation codes, it is important to have a detailed understanding of rate coefficients, cross sections, and collisional dynamics for fundamental processes in both the plasma phase and on surfaces. Plasma plumes produced by plasma jet devices expand into the air around them and can be up to several centimeters long. Additionally, the gas stream also maintains its ambient temperature [24].

To utilize and adjust the plasma jet in a limited way for applications, some characterization of the plasma jet, such as electron temperature (T_e) and electron density (n_e), must be carried out thoroughly. Previously, this information on plasma jets has been received using Rayleigh scattering [25], Thomson scattering [26], time-resolved fast imaging [27], optical emission spectra (OES) [28][29], etc.

In general, OES offers purposive and easy-to-implement measurements for plasma diagnosis. OES will cover a range of wavelengths between 200 and 1200 nm. This method relies on the involution of Gaussians, Lorentzians, and Stark profiles to achieve the stark broadening of the plasma spectral line [30]. Charged particles interacting with neutral atoms cause the Stark broadening of lines [31]. Atoms in diverse positions in the plasma are impacted by various electric fields that change over time due to relative motion of the charged particles and atoms. The perturbation of the electric field affects slightly the optical transitions' selection and the atomic level's degeneracy (Stark effect) [32]. Therefore, these changes result in an alteration of the line width, shape, and position. The controlling interaction of the atom is the stark effect in the plasma situation, where the ratio of charged particles to neutral atoms is greater. Thus, the measurement of stark broadening of the plasma spectral line is an ideal tool for determining the electron density ($\mathbf{n_e}$) which is given by [33].

$$\mathbf{n_e(cm^{-3})} = \left(\frac{\Delta\lambda}{2\omega_s\,(\lambda,T_e)}\right)N_r \qquad (1)$$

Where $\Delta\lambda$ is the full width half maximum (FWHM) of the line, ω_s is the stark broadening parameter, and N_r is the reference electron density.

In local thermodynamic equilibrium (**LTE**), a Boltzmann distribution is achieved between energy levels, while the radiation is not in thermal equilibrium. The collisional transition should be greater than the radiative transitions for achieving LTE, so it is performed only in high-density plasmas [34]. For plasmas in LTE, the electron temperature is defined as follows [35]:

$$ln\ ln\left(\frac{I_{ji}\,\lambda_{ji}}{h\,c\,A_{ji}\,g_j}\right) = \left(-\frac{E_j}{kT_e}\right) + ln\left(\frac{N}{U(T)}\right) \qquad (2)$$

Where N is the total population density, U(T) partition function, $\mathbf{E_j}$ excitation energy of one level (in **eV**), k Boltzmann constant (1.38×10^{-23} J/K), $\boldsymbol{\lambda_{ji}}$ wavelength corresponding to the transmission between level j and level i, I_{ji} spectral line intensity, g_j the density of states, and A_{ji} transition probability between the upper-level j and lower-level i.

ISSN: 1814-635X (print), ISSN:2521-3520 (online) Volume 34, Issue 3, 2023 DOI: http://doi.org/10.23851/mjs.v34i3.1369

A significant plasma property is the stability of its macroscopic area charge neutrality. A high electric field induces collective particle motions that restore the initial charge neutrality when plasma is abruptly disturbed from the equilibrium condition [36]. These motions are described by an intrinsic frequency of oscillation called plasma frequency, which is given by [37]:

$$\mathbf{f_p} = \sqrt{\frac{n_e\, e^2}{m_e \varepsilon_0}} / \mathbf{2\pi} = \mathbf{8.89}\sqrt{n_e} \qquad (3)$$

Where, $\mathbf{n_e}$ is the electron density, **e** is the elementary charge, $\mathbf{m_e}$ is the electron mass, and $\boldsymbol{\varepsilon}_\circ$ is the permittivity of the vacuum.

The Debye length is another physical parameter for the characterization of plasma. It allows a measure of the distance over which ions and electrons can be separated in plasma. The arrangement of the electrons and ions successfully shields any electrostatic forces at a distance of the Debye length ($\boldsymbol{\lambda_D}$) [38][39]. It can be expressed as:

$$\boldsymbol{\lambda_D} = \left(\frac{\varepsilon_0\, k\, T}{n_e\, e^2}\right)^{\mathbf{1/2}} \qquad (4)$$

Since only the charged particles that are located inside the Debye sphere interact collectively with each other in plasma physics, the number of electrons (N_D) inside the Debye sphere is given by [37]:

$$\mathbf{N_D} = \frac{4}{3}\,\pi\,\boldsymbol{\lambda_D}^3\,\mathbf{n_e} \qquad (5)$$

The effect of changing potential discharge on the intensity of the spectral lines in Ar/O_2 plasma discharge is studied to determine the optimum condition of produced plasma.

MATERIALS AND METHODS

Experimental Setup

This study reveals the discharge control settings that have the greatest impact on the plasma stream's length and properties outside. The mixture of gases was studied to determine the best properties of cold atmospheric plasma based on different voltages. Figure 1 illustrates the experimental setup used for cold atmospheric plasma (CAP) generation. The CAP jet consists of a 10 cm long quartz tube with a 7 mm inner and 10 mm outer diameter through which an Ar/O_2 mixture gas flow was applied. An aluminum ring (10 mm in width) was wrapped around a quartz tube as a ground electrode with a distance of 5 mm to the orifice of the tube, and a copper wire inside the quartz tube represents a high-voltage electrode. Argon (Ar) was utilized as the vector gas with an adjusted flow rate of 15 l/min and oxygen (O_2) was used as the reactive gas with a flow rate of 1.5 l/min in this experiment. The discharge was obtained by applying a high-voltage AC power supply (**Fanavaran Nano- Meghyas HV35P OV**), and it was adjusted in this experiment between 14 kV and 18 kV. As the potential discharge increases, the plasma plume's length rises from 1.5 cm to 4 cm. The optical emission spectroscopy (OES) from the CAP jet was collected by an (**Ocean Optics spectrometer, Flame-S-XR1**) using a fiber probe. A distance of 0.5 cm was used to measure the plasma optical emissions from the plasma plume. The recorded spectrum was examined in accordance with the atomic spectra database lines (NIST), and as a result, the plasma parameters were identified.

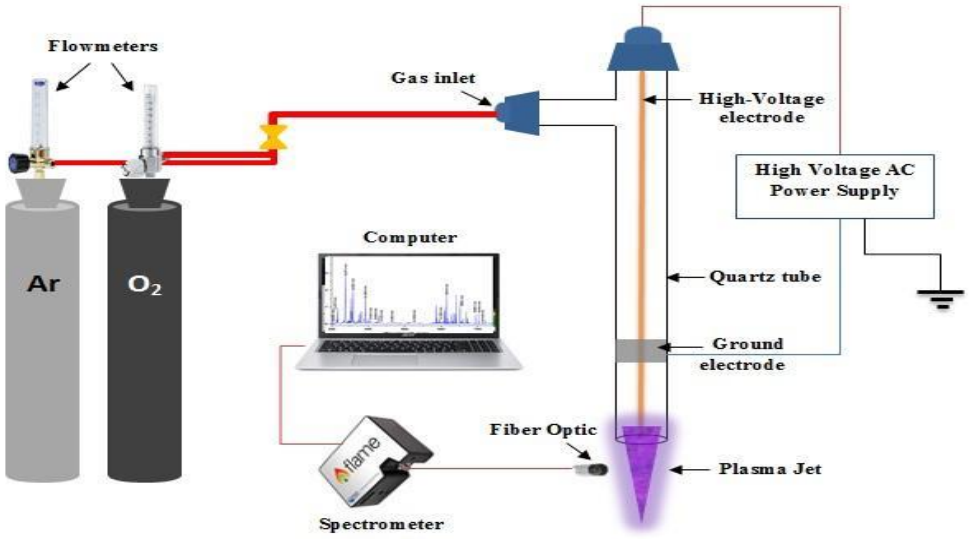

Figure 1: Schematic diagram of cold atmospheric plasmas (CAPs).

RESULTS AND DISCUSSION

This study examines how the most crucial plasma plume parameters discharge, voltage, and mixed gas affect the lengthy and brilliant plasma plume. With varied potential discharges of 14 kV, 16 kV, and 18 kV, the OES spectrum was captured from the plasma jet produced by cold atmospheric plasma. Ar/O_2 between 200 nm and 1000 nm was used for the analysis of the discharge.

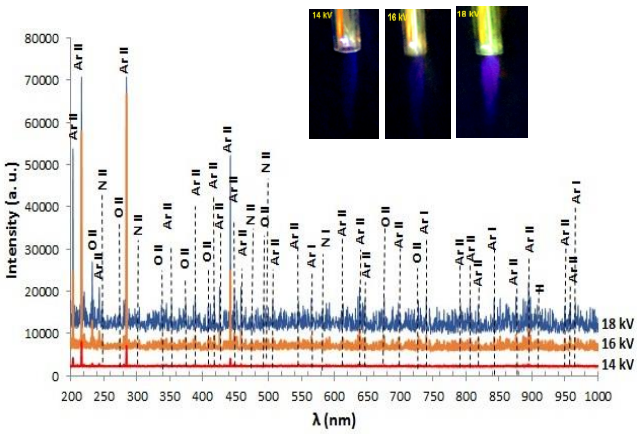

Figure 2: Emission spectra of cold atmospheric plasmas (CAPs) for Ar/O2 mixture gas with different potential discharges (the inset represents cold plasma at 14, 16, and 18 kV).

Figure 2 shows the strong peaks were primarily acquired in the UV/visible area; However, there were no clearly defined peaks in the near-infrared region. Moreover, the optical emission spectrum had argon emission lines predominating it, which was expected given that argon makes up the majority of the mixture gas and oxygen only makes up 10% of the whole gas, according to comparison results with the NIST Atomic spectra database. In detail, the strong and main atomic argon was visible at around (203, 216, 284, and 442) nm, corresponding to the argon atom transitions of ArII ($3s^2\ 3p^4\ (^3P)\ 4f \rightarrow 3s^2\ 3p^4\ (^3P_2) 3d$), ArII ($3s^2\ 3p^4\ (^1D)\ 4f \rightarrow 3s^2\ 3p^4\ (^3P_2)\ 4s$), ArII ($3s^2\ 3p^4\ (^3P)\ 4p \rightarrow 3s^2\ 3p^4\ (^1D)\ 4s$), and ArII ($3s^2\ 3p^4\ (^3P)\ 4p \rightarrow 3s^2\ 3p^4\ (^3P)\ 4s$), respectively. Equally significant is the distinct atomic oxygen that is the dominant reactive component in the gas emissions at around (232 and 411) nm, corresponding to the oxygen atom transitions of:
OII ($2s^2\ sp^2\ (^3P)\ 4d \rightarrow 2s^2\ 2p^2\ (^3P)\ 3p$) and
OII ($2s^2\ 2p^2\ (^3P)\ 3d \rightarrow 2s^2\ 2p^2\ (^3P)\ 3p$), respectively. The atomic oxygen in the plasma was produced as a result of the dissociation of O molecules by Ar metastable ($Ar^* + O_2 \rightarrow O\ (3p\ ^3P) + O + Ar$) or electrons ($e^- + O_2 \rightarrow O\ (3p\ ^3P) + O + e^-$). However, from the emission spectral results noticed that the increase of discharge potential effected the intensity of the excited species.
Figure 3 shows the electron temperature (T_e) was calculated by Boltzmann plot taking four lines of ArII lines at (284.53, 418, 439.59, 442.66) nm. The electron temperature (T_e) values were calculated by plotting between $ln\ ln\ (\frac{I_{ji}\ \lambda_{ji}}{h\ c\ A_{ji}\ g_j})$ versus the upper energy level

(E_j). The equation of the fitting and the R^2 are illustrated in the figure. R^2, a statistical coefficient, measures the accuracy of the linear fit and ranges in value from (0-1).

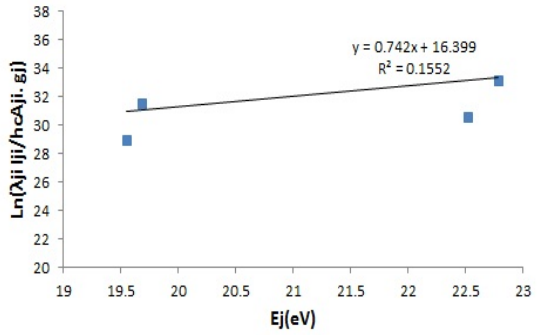

(a)

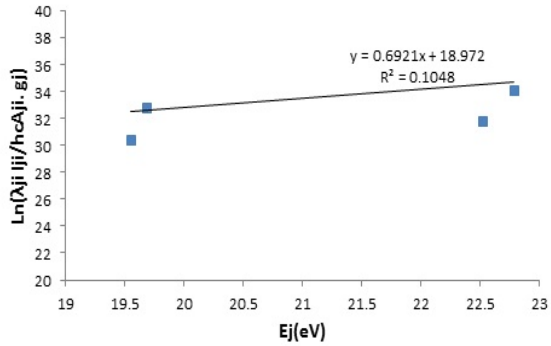

(b)

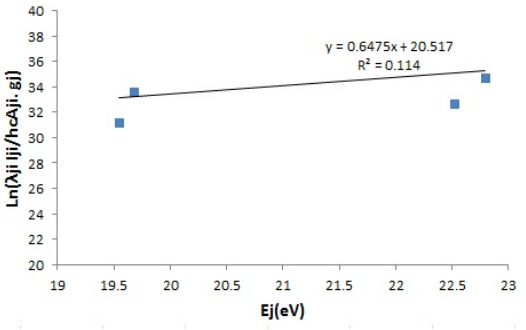

(c)

Figure 3: Boltzmann plot for cold atmospheric plasmas (CAPs) at different potential discharges: (a) 14 kV, (b) 16kV, and (c) 18 kV.

As can be seen in Figure 4, when the potential discharge intensifies from 14 kV to 18 kV, both the electron temperature (T_e) and the electron density (n_e) increase.

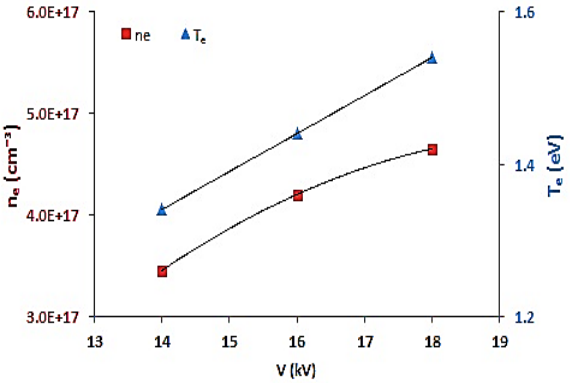

Figure 4: Variation of (T_e) and (n_e) versus the potential discharges (14, 16, and 18 kV).

The electron temperature (T_e) increases from (1.34 to 1.54) eV, while the electron density (n_e) increases from ($3.5*10^{17}$ to $4.7*10^{17}$) cm^{-3}. This is due to the increase in kinetic energy of the electrons caused by the higher potential discharge, which in turn results in an increase of electron temperature (T_e) and electron density (n_e). Table 1 illustrates the electron plasma temperature (T_e), electron plasma density (n_e), plasma frequency (f_p), Debye length (λ_D), and number of particles in the Debye sphere (N_D) of cold atmospheric plasma at the potential discharge voltages of 14 kV, 16 kV and 18 kV. Criteria plasma is satisfied, exhibiting a decrease in λ_D with increased potential discharge due to its proportionality to electron density (n_e). At the same time, f_p and N_D showed an upward trend with increasing potential discharge.

Table 1 Plasma parameters for cold atmospheric plasmas (CAPs) with different potential discharges.

V (kV)	T_e (eV)	FWHM	$n_e*10^{17}(cm^{-3})$	$f_p*10^{12}(Hz)$	$\lambda_D*10^{-5}(cm)$	N_D*10^3
14	1.34	0.460	3.5	5.3	1.464	4.5
16	1.44	0.56	4.2	5.8	1.375	4.6
18	1.54	0.62	4.7	6.1	1.352	4.8

CONCLUSIONS

The Optical Emission Spectroscopy technique (OES) proves to be adequate for determining plasma characteristics. Our exploration has focused on how various potential discharges affect the plasma characteristics of cold atmospheric plasmas (CAPs). We have observed a significant impact on emission intensity due to changes in potential discharge at constant flow rates, implying an increase in the

number of ionized particles. This observation suggests that the majority of molecules passing through the plasma tube become ionized, owing to the sufficient energy supplied by the potential discharge, leading to secondary ionization of the molecules.

Consequently, the plasma state is influenced by the potential discharge, resulting in the intensity appearing to reach its lowest point at 14 kV and its highest point at 18 kV. This leads us to the conclusion that an increase in potential discharge substantially affects the density and temperature of electrons as well as other plasma characteristics. As the potential discharge increases, the plasma frequency decreases, the number of particles on the surface of the Debye sphere diminishes, and the Debye length increases.

Disclosure and Conflicts of Interest: The authors advertise that they have no conflicts of interest.

REFERENCES

[1] A. Ansari, K. Parmar, M. Shah, "A comprehensive study on decontamination of food-borne microorganisms by cold plasma", *Food Chemistry: Molecular Sciences*, vol. 4, 2022. https://doi.org/10.1016/j.fochms.2022.100098

[2] K. Jenns, H. P. Sassi, R. Zhou, P. J. Cullen, D. Carter, A. M. Prochnow, "Inactivation of foodborne viruses: Opportunities for cold atmospheric plasma", *Trends in Food Science & Technology*, vol. 124, 2022, pp. 323-333. https://doi.org/10.1016/j.tifs.2022.04.006

[3] Z. Chen, G. Chen, R. Obenchain, R. Zhang, F. Bai, T. Fang, H. Wang, Y. Lu, R. E. Wirz, Z. Gu, "Cold atmospheric plasma delivery for biomedical applications", *materialstoday*, vol. 54, 2022, pp. 153-188. https://doi.org/10.1016/j.mattod.2022.03.001

[4] M. Mohammed., B. M. Ahmed, "Effect of Colloidal Cu NPs/Cinnamon Extract on the Antibacterial Activity", *Al-Mustansiriyah Journal of Science*, vol. 33, 2022, pp. 94-99. https://doi.org/10.23851/mjs.v33i4.1154

[5] R. M. Sankaran, "Plasma Processing of Nanomaterials", *CRC Press: Taylor & Francis Group*, Boca Raton London New York, 2012.

[6] R. Chang, N. Ji, M. Li, L. Qiu, C. Sun, X. Bian, H. Qiu, L. Xiong, Q. Sun, "Green preparation and characterization of starch nanoparticles using a vacuum cold plasma process combined with ultrasonication treatment", *Ultrasonics Sonochemistry*, 2019. https://doi.org/10.1016/j.ultsonch.2019.10

[7] Q. Zhang, W. Yang, S. Zhang, J. Tang, X. Shi, S. Qin, "Enhancing the applicability of gelatin-carboxymethyl cellulose films by cold plasma modification for the preservation of fruits", *LWT - Food Science and Technology*, vol. 178, 2023. https://doi.org/10.1016/j.lwt.2023.114612

[8] A. Rafique, Y. E. Bulbul, A. Usman, Z. A. Raza, A. U. Oksuz, "Effect of cold plasma treatment on polylactic acid and polylactic acid/poly (ethylene glycol) films developed as a drug delivery system for streptomycin sulfate", *International Journal of Biological Macromolecules*, vol. 235, 2023. https://doi.org/10.1016/j.ijbiomac.2023.123857

[9] Da. Mei, X. Shen, S. Liu, R. Zhou, X. Yuan, Z. Rao, Y. Sun, Z. Fang, X. Du, Y. Zhou, X. Tu, "Plasma-catalytic reforming of biogas into syngas over Ni-based bimetallic catalysts", *Chemical Engineering Journal*, vol. 462, 2023. https://doi.org/10.1016/j.cej.2023.142044

[10] Y. Song and X. Fan, "Hydrogen Peroxide Residue on Tomato, Apple, Cantaloupe, and Romaine Lettuce after Treatments with Cold Plasma–Activated Hydrogen Peroxide Aerosols", *Journal of Food Protection*, vol. 84, 2021, pp. 1304–1308. https://doi.org/10.4315/JFP-21-051

[11] U.G. M. Ekanayake, D. H. Seo, K. Faershteyn, A. P. O'Mullane, H. Shon, J. MacLeod, D. Golberg, K. (Ken) Ostrikov, "Atmospheric-pressure plasma seawater desalination: Clean energy, agriculture, and resource recovery nexus for a blue planet", *Sustainable Materials and Technologies*, vol. 25, 2020. https://doi.org/10.1016/j.susmat.2020.e00181

[12] X. Lu, G. V. Naidis, M. Laroussi, S. Reuter D. B. Graves, K. Ostrikov, "Reactive Species in Non-equilibrium Atmospheric-Pressure Plasmas: Generation, Transport, and Biological Effects", *Physics Reports*, vol. 630, 2016, pp. 1-84. https://doi.org/10.1016/j.physrep.2016.03.003

[13] M. Keidar, D. Yan, J. H Sherman, "Cold Plasma Cancer Therapy", *Morgan & Claypool Publishers*, 2019.

[14] P. Ji, H. Jin, D. Li, X. Su, B. Wang, " Thermal analysis of inductively coupled atmospheric pressure plasma jet and its effect for optical processing", *Optik*, vol. 185, 2019, pp. 381-389. https://doi.org/10.1016/j.ijleo.2019.03.098

[15] G. Faingold, J. K. Lefkowitz, "A numerical investigation of NH3/O2/He ignition limits in a non-thermal plasma", *Proceedings of the Combustion Institute*, vol. 38, 2021, pp. 6661-6669. https://doi.org/10.1016/j.proci.2020.08.033

[16] M. Hosseinpour, A. Zendehnam, S. M. H. Sangdehi, H. G. Marzdashti, " Effects of different gas flow rates and non‐perpendicular incidence angles of argon cold atmospheric‐pressure plasma jet on silver thin film treatment", *Journal of Theoretical and Applied Physics*, vol. 13, 2019, pp. 329–349. https://doi.org/10.1007/s40094-019-00351-7

[17] D. Cui, Y. Yin, H. Sun, X. Wang, J. Zhuang, L. Wang, R. Ma, Z. Jiao, " Regulation of cellular redox homeostasis in Arabidopsis thaliana seedling by atmospheric pressure cold plasma-generated reactive oxygen/nitrogen species", *Ecotoxicology and Environmental Safety*, vol. 240, 2022. https://doi.org/10.1016/j.ecoenv.2022.113703

[18] Y. Yang, M. Zheng, Y. N. Jia, J. Li, H. P. Li, J. G. Tan, " Time-dependent reactive oxygen species inhibit Streptococcus mutans growth on zirconia after a helium cold atmospheric plasma treatment", *Materials Science and Engineering: C*, vol. 120, 2021. https://doi.org/10.1016/j.msec.2020.111633

[19] P. Lamichhane, T. R. Acharya, N. Kaushik, L. N. Nguyen, J. S. Lim, V. Hessel, N. K. Kaushik, E. Ha. Choi, "Non-thermal argon plasma jets of various lengths for selective reactive oxygen and nitrogen species production", *Journal of Environmental Chemical Engineering*, vol. 10, 2022. https://doi.org/10.1016/j.jece.2022.107782

[20] A. Barjasteh, Z. Dehghani, P. Lamichhane, N. Kaushik, E. H. Choi, N. K. Kaushik, "Recent Progress in Applications of Non-Thermal Plasma for Water Purification, Bio-Sterilization, and Decontamination", *applied sciences*, vol. 11, 2021. https://doi.org/10.3390/app11083372

[21] P. Attri, Y. H. Kim, D. H. Park, J. H. Park, Y. J. Hong, H. S. Uhm, K. N. Kim, A. Fridman, E. H. Choi, "Generation mechanism of hydroxyl radical species and its lifetime prediction during the plasma-initiated ultraviolet (UV) photolysis", *Scientific Reports*, vol. 5(1), 2015. https://doi.org/10.1038/srep09332

[22] Y. Li, M. H. Kang, H. S. Uhm, G. J. Lee, E. H. Choi, I. Han, " Effects of atmospheric-pressure non-thermal bio-compatible plasma and plasma activated nitric oxide water on cervical cancer cells", *Scientific Reports*, vol. 7, 2017. https://doi.org/10.1038/srep45781

[23] P. Lamichhane, R. Paneru, L. N. Nguyen, J. S. Lim, P. Bhartiya, B. C. Adhikari, S. Mumtaz, E. H. Choi, " Plasma-assisted nitrogen fixation in water with various metals", *Reaction Chemistry & Engineering*, 2020. https://doi.org/10.1039/D0RE00248H

[24] Q. Xiong, X. Lu, K. Ostrikov, Z. Xiong, Y. Xian, F. Zhou, C. Zou, J. Hu, W. Gong, and Z. Jiang, "Length control of He atmospheric plasma jet plumes: Effects of discharge parameters and ambient air", *Physics of Plasmas*, vol. 16, 2009. https://doi.org/10.1063/1.3119212

[25] A. G. Carbone, P. J. Bruggeman, J. d. Mullen, " Laser scattering on an atmospheric pressure plasma jet: disentangling Rayleigh, Raman and Thomson scattering", *Plasma Sources Science Technology*, vol. 21, 2012. https://10.1088/0963-0252/21/1/015003

[26] S. Hübner, J. S. Sousa, V. Puech, G. M. Kroesen, N. Sadeghi, "Electron properties in an atmospheric helium plasma jet determined by Thomson scattering", *Journal of Physics D Applied Physics*, vol. 47(43), 2014. https://10.1088/0022-3727/47/43/432001

[27] E. Simoncelli, A. Stancampiano, M. Boselli, M. Gherardi, V. Colombo, "Experimental Investigation on the Influence of Target Physical Properties on an Impinging Plasma Jet", *Plasma*, vol. 2, 2019, pp. 369–379. https://doi.org/10.3390/plasma2030029

[28] B. field , R. Scott, "Optical Emission Spectroscopy of High Voltage Cold Atmospheric Plasma Generated Using Dielectric Barrier Discharges" Open Access Theses, 2016.

[29] J. Mrotzek, W. Viöl, "Spectroscopic Characterization of an Atmospheric Pressure Plasma Jet Used for Cold Plasma Spraying", *applied sciences*, vol. 12, 2022. https://doi.org/10.3390/app12136814

[30] A. D. Soriano, J. M. A. Pelegrina, A. Sarsa, M. S. Dimitrijević, C. Yubero, " A simple and accurate analytical model of the Stark profile and its application to plasma characterization", *Journal of Quantitative Spectroscopy and Radiative Transfer*, vol. 207, 2018, pp. 89-94. https://doi.org/10.1016/j.jqsrt.2017.12.027

[31] E. Oks, "Stark Broadening of Spectral Lines in Plasmas", *Printed Edition of the Special Issue Published in Atoms*, 2018.

[32] A. Y. Nikiforov, C. Leys, M. A. Gonzalez, J. L. Walsh, " Electron density measurement in atmospheric pressure plasma jets: Stark broadening of hydrogenated and non-hydrogenated lines", *Plasma Sources Science Technology*, vol. 24, 2015. https://10.1088/0963-0252/24/3/034001

[33] B. M. Ahmed, S. H. A. Muslim, M. J. Khoudair, " Determine emissions plasma Iron by Laser-Induced Breakdown spectroscopic in Atmospheric environment", *Minar International Journal of Applied Sciences and Technology*, vol. 2(4), 2020, pp. 100–106. https://www.minarjournal.com/dergi/determine-emissions-plasma-iron-by-laser-induced-breakdown-spectroscopy-in-atmospheric-environment20210407052857.pdf

[34] X. Bai, "Laser-induced plasma as a function of the laser parameters and the ambient gas", *Université Claude Bernard - Lyon I*, 2014.

[35] M. A. Khalaf, B. M. Ahmed, K. A. Aadim, "Spectroscopic Analysis of CdO_{1-x}: Sn_x Plasma produced by Nd: YAG Laser", *Iraqi Journal of Science*, vol. 61(7), 2015, pp. 1665-1671. https://ijs.uobaghdad.edu.iq/index.php/eijs/article/view/2188

[36] J.A. Bittencourt, "Fundamentals of Plasma Physics", Third Edition, *Springer Science & Business Media New York*, 2004.

[37] F. F. Chen, "introduction to plasma physics and controlled fusion", Third edition, *Springer international publication Switzerland*, 2016.

[38] B. M. Ahmed, R. A. Abdulrazaq, M. A. Khalaf, O. A. A. Dakhil, "Parameters for Fe_2O_3 On Staphylococcus Aureus and Acinetobacter Baumannil", *Journal of Engineering Science and Technology*, vol. 17, 2022, pp. 0552 – 0562. https://jestec.taylors.edu.my/Vol%2017%20Issue%201%20February%20%202022/17_1_38.pdf

[39] B. M. Ahmed, "Plasma parameters Generated from Iron Spectral Lines by using LIBS Technique", *IOP Conf. Series: Materials Science and Engineering*, 2020. https://iopscience.iop.org/article/10.1088/1757-899X/928/7/072096/pdf

How to Cite

R. A. S. Alkareem, B. M. . Ahmed, O. A. A. . Dakhil, and A. . Albeer, "Plasma Parameters Diagnosis of Laboratory Ar/O2 Cold Atmospheric Plasma Jet using Different Potential Discharges", *Al-Mustansiriyah Journal of Science*, vol. 34, no. 3, pp. 124–131, Sep. 2023.